

Synthesis of Granular Free- Binder ZSM-5 Zeolites with a Hierarchical Porous Structure Using Different Amorphous Aluminosilicates

[Alina Kh. Ishkildina](#) , [Olga S. Travkina](#) , [Dmitry V. Serebrennikov](#) ^{*} , [Rufina A. Zilberg](#) , [Artur I. Malunov](#) , [Nadezhda A. Filippova](#) , [Boris I. Kutepov](#) , [Marat R. Agliullin](#)

Posted Date: 25 December 2024

doi: 10.20944/preprints202412.2161.v1

Keywords: ZSM-5 zeolite; amorphous aluminosilicate; hierarchical porous structure; granular zeolite; hydrocracking of n-paraffins



Preprints.org is a free multidisciplinary platform providing preprint service that is dedicated to making early versions of research outputs permanently available and citable. Preprints posted at Preprints.org appear in Web of Science, Crossref, Google Scholar, Scilit, Europe PMC.

Copyright: This open access article is published under a Creative Commons CC BY 4.0 license, which permit the free download, distribution, and reuse, provided that the author and preprint are cited in any reuse.

Article

Synthesis of Granular Free- Binder ZSM-5 Zeolites with a Hierarchical Porous Structure Using Different Amorphous Aluminosilicates

Alina Kh. Ishkildina ¹, Olga S. Travkina ¹, Dmitry V. Serebrennikov ^{1,*}, Rufina A. Zilberg ², Artur I. Malunov ¹, Nadezhda A. Filippova ¹, Boris I. Kutepov ¹ and Marat R. Agliullin ¹

¹ Institute of Petrochemistry and Catalysis, Ufa Federal Research Centre of the Russian Academy of Sciences (UFRS RAS), 450075 Ufa, Russia

² Department of Analytical Chemistry, Ufa University of Science and Technology, 450076 Ufa, Russia

* Correspondence: d25c25@yandex.ru (D.V.S.)

Abstract: In this paper we discuss options for the synthesis of granular free- binder ZSM-5 zeolites using synthetic aluminosilicates prepared by sol-gel technology with organic and inorganic silicon sources. It has been shown that the properties of the amorphous aluminosilicate used to prepare the initial granules influence the crystallization conditions as well as the morphology and size of the crystals formed from granular ZSM-5 zeolite. We propose promising catalytic systems for the hydrocracking of n-paraffins based on granular zeolite ZSM-5 with a hierarchical porous structure.

Keywords: ZSM-5 zeolite; amorphous aluminosilicate; hierarchical porous structure; granular zeolite; hydrocracking of n-paraffins

1. Introduction

Currently, zeolites are widely used in the production of modern adsorbents and catalysts for the petrochemical and oil refining industries due to their successful combination of microporous structures, strong acid sites, molecular sieving effects and high hydrothermal and thermal stability [1,2]. Among the various types of molecular sieves, ZSM-5 zeolite is the most widely used in catalytic systems. It belongs to the MFI structural type and has a three-dimensional porous structure consisting of rectangular and elliptical channels with dimensions of $5.3 \times 5.6 \text{ \AA}$ and $5.1 \times 5.5 \text{ \AA}$, respectively [3].

The main efforts of researchers in the field of ZSM-5 zeolite synthesis have focused on the development of methods for the preparation of nanoscale and hierarchical crystals in order to overcome the diffusion limitations in their micropores [4–10]. It has been demonstrated that catalytic systems based on these nanoscale and hierarchical ZSM-5 zeolite crystal structures exhibit higher activity, selectivity and stability in several industrially important catalytic processes [11–15].

Unfortunately, most methods for the synthesising these materials rely on the use of crystal growth modifiers and pore-forming templates. However, the main drawback of these methods for producing nanoscale and hierarchical zeolite crystals, such as ZSM-5 zeolite, is their high cost, which makes them unsuitable for large-scale industrial production.

In industrial processes, zeolite-based catalysts such as ZSM-5 are used in granular form. These granules are produced by mixing and pelletising powdered zeolite with boehmite, followed by drying at temperatures between 120–150°C and calcining at temperatures between 500–650°C. During this process, boehmite is transformed into $\gamma\text{-Al}_2\text{O}_3$ [16,17]. During granulation, the pores of the zeolite crystals may be partially blocked by a binder. The amount of binder used depends on the amount of Al_2O_3 present in the mixture [16,17].

In [18], a method for the preparation of granular ZSM-5 zeolite without the use of binders was proposed. This method involves crystallizing the granules at 180°C for 24 h in a 0.01 M NaOH solution, using dried aluminosilicate gel granules prepared with sodium silicate as a temporary binder. It has been shown that this approach allows for the synthesis of granular ZSM-5 zeolite without the

use of binders. However, it should be noted that this study does not provide information on the mechanical strength of the granules, which is a critical parameter for industrial catalysts.

In [19], a method was proposed for the synthesis of granular zeolite NaY with a hierarchical porous structure was proposed. The method involves the crystallization of granules consisting of Y zeolite and metakaolin ($\text{SiO}_2/\text{Al}_2\text{O}_3 = 2.0\text{-}2.21$), which during the crystallization process are transformed into individual clusters of crystals, including nanoscale crystals. This approach has made it possible to obtain granular materials with a high degree of crystallinity without binders, with a hierarchical (micro-, meso-, macroporous) porous structure. However, the use of kaolin for the preparation of zeolites with a molar $\text{SiO}_2/\text{Al}_2\text{O}_3$ ratio higher than 30 is not promising, due to its low silicon content.

Therefore, the aim of this study is to develop a method for the synthesis of granular binder-free ZSM-5 zeolites using amorphous aluminosilicates obtained by the sol-gel process as a temporary binder.

2. Materials and Methods

2.1. Synthesis of Powdered ZSM-5 Zeolite

Highly dispersed Na-ZSM-5 zeolite with a $\text{SiO}_2/\text{Al}_2\text{O}_3$ ratio of 50 was obtained by hydrothermal crystallization in Teflon-coated autoclaves at 160 °C for 48 h from an amorphous alkaline aluminosilicate with the following composition: $0.03\text{Na}_2\text{O} \cdot 0.04\text{TBABr} \cdot 0.02\text{Al}_2\text{O}_3 \cdot 1.00\text{SiO}_2 \cdot 16.00\text{H}_2\text{O}$ prepared by mixing solutions of sodium silicate ($\text{Na}_2\text{O}(\text{SiO}_2)_x \cdot x\text{H}_2\text{O}$, No. CAS 6834-92-0, Sigma-Aldrich) and sodium aluminate (No. CAS 11138-49-1, Sigma-Aldrich), ground silica gel (No. CAS 112926-00-8, Sigma-Aldrich), and an organic template - tetrabutylammonium bromide (TBABr, No. CAS 1643-19-2, Sigma-Aldrich).

The crystallization products were separated by centrifugation and washed with distilled water until the pH was neutral. They were then dried at 150°C for 8-10 h. The resulting powdered zeolite was named NaZSM-5 sample.

2.2. Synthesis of Amorphous Aluminosilicates

An amorphous aluminosilicate (molar ratio of $\text{SiO}_2/\text{Al}_2\text{O}_3 = 50$) was synthesized using an organic silicon source by a two-stage sol-gel method, following the procedure described in [20]. In the first stage, a calculated amount of distilled water and ethanol ($\text{C}_2\text{H}_5\text{OH}$, 99%, No. CAS 64-17-5, Sigma-Aldrich) was added to tetraethyl orthosilicate (TEOS, 99%, No. CAS 78-10-4, Sigma-Aldrich), with intensive stirring. Aluminium nitrate ($\text{Al}(\text{NO}_3)_3 \cdot 9\text{H}_2\text{O}$, 98%, No. CAS 7784-27-2, Sigma Aldrich) was then added to the resulting solution. The resulting solution with a pH of approximately 3 was then kept in a thermostat at 60°C for 25 h, until the gelation point was reached. An aqueous solution of ammonia (NH_4OH , 30%, No. CAS 1336-21-6, Sigma Aldrich) was then added to the resulting gel, with vigorous stirring, until a pH of 10 was reached. The mixture was then aged at 25°C for a further 24 h. Finally, the gel was dried at 120°C for 5 h to obtain the final product. The resulting amorphous aluminosilicate was named ASM-1 sample.

An amorphous aluminosilicate with a molar ratio of $\text{SiO}_2/\text{Al}_2\text{O}_3 = 50$ was synthesized using an inorganic silicon source. The synthesis process involved mixing aqueous solutions of sodium silicate and aluminium sulfate ($\text{Al}_2(\text{SO}_4)_3 \cdot 18\text{H}_2\text{O}$, 99%, No. CAS 7784-31-8, Sigma-Aldrich) to form a gel. The gel was then aged for 24 h at 25 °C, then filtered and washed with distilled water to remove any impurities. After this washing step, the amorphous aluminosilicate was dried at 120 °C for 5 h. The final product of this process, called the ASM-2 sample, is an amorphous material with the desired molar ratio.

2.3. Preparation of Granules Containing Zeolite ZSM-5 and Amorphous Aluminosilicates

The initial granules were prepared by combining powdered NaZSM-5 zeolite and amorphous aluminosilicates in a mixer (VINCI Technologies MX 0.4). The resulting mixture was moistened with a solution of polyvinyl alcohol (99%, No. CAS 9002-89-5, Sigma Aldrich) to form granules with a

diameter of 1.4-1.6 millimeters and a length of 5-6 millimeters. The granules were then formed on an extruder (VINCI Technologies VTE1).

The content of powdered ZSM-5 zeolite and amorphous aluminosilicate in the granules was 60% and 40% by weight, respectively. The granules obtained using the amorphous aluminosilicates ASM-1 and ASM-2 were further designated as NaZSM-5-ASM-1 and NaZSM-5-ASM-2 zeolites, respectively.

2.4. Preparation of Granules Containing ZSM-5 Zeolite and Boehmite

Granular ZSM-5 zeolite in the Na form, with a binder, was prepared as follows: The NaZSM-5 sample and boehmite ($\text{AlO}(\text{OH})$, 78% Al_2O_3 , No. CAS 1318-23-6, Sasol) were thoroughly mixed in a mixer to obtain a homogeneous mixture. The content of boehmite in the granules, expressed as Al_2O_3 , was 30% by weight.

The resulting mixture was wetted with a 5% nitric acid (HNO_3 , 67%, No. CAS 7697-37-2, Reachem) solution and extruded into granules (diameter: 1.4–1.6 mm, length: 5–6 mm) using an extruder. The granules were then dried at 150 °C for 24 h and calcined at 500–600 °C for 6 h to convert boehmite to $\gamma\text{-Al}_2\text{O}_3$. The sample obtained by this method is designated as NaZSM-5-BD.

2.5. Preparation of Granular Binder-Free ZSM-5 Zeolites

Granular NaZSM-5-ASM-1 and NaZSM-5-ASM-2 zeolites were crystallized in a solution of sodium silicate. The concentrations of sodium and silicon were chosen on the basis of the composition of the reaction mixture (RM): 2.3R: 3.2 Na_2O : Al_2O_3 : 60 SiO_2 : 550 H_2O (R - organic template, tetrabutylammonium bromide).

The granules were stored at room temperature for 1-32 h prior to crystallization. Crystallization was performed in Teflon-lined autoclaves. The temperature for crystallization was 160 °C and the duration was 48 h. After the crystallization process, the samples were washed to remove any residual components from the mother liquor, then dried at 120 °C for 5-6 h, and finally calcined at 600 °C for 3-4 h to remove the template.

The samples obtained by crystallization from the NaZSM-5-ASM-1 and NaZSM-5-ASM-2 samples are designated as NaZSM-5-WB-1 and NaZSM-5-WB-2, respectively.

2.6. Preparation of H-Form Zeolites

The H-form of the powder and granular samples was obtained after crystallization by ion exchange of Na^+ cations with NH_4^+ cations in an aqueous solution of ammonium nitrate (NH_4NO_3 , 98%, No. CAS 6484-52-2, Sigma Aldrich) at 70 °C for 1 h with stirring. The granules were then dried at 120 °C and calcined at 550 °C for 4 h in an air atmosphere. The H-form samples were assigned an H-index.

2.7. Preparation of a Bifunctional Catalyst

Fractions of 0.1 to 0.5 mm were obtained from HZSM-5-WB-1, HZSM-5-WB-2, and HZSM-5-BD samples by grinding and passing through sieves. This material was then heat treated at 350 °C for 6 h in air. The catalyst was then impregnated with an aqueous solution of $\text{H}_2\text{PtCl}_6 \times 6\text{H}_2\text{O}$ (99%, No. CAS 26023-84-7, Sigma Aldrich) at a concentration of 0.5% wt/wt of Pt per support weight. The catalyst was then dried at 100 °C for 24 h and calcined at 550 °C for 5 h. Prior to the reaction, the catalyst was reduced in a hydrogen atmosphere at 400 °C for 5 h. Samples containing 0.5% Pt were designated as Pt/ZSM-5-WB-1, Pt/ZSM-5-WB-2, and Pt/ZSM-5-BD.

2.8. Zeolite Research Methods

The chemical composition of the samples was determined using a Shimadzu EDX-7000P spectrometer manufactured by Shimadzu Corporation.

The phase composition and crystallinity of the samples were determined by X-ray diffraction using a Shimadzu XRD 7000 diffractometer with $\text{CuK}\alpha$ radiation. Scanning was performed in the

range of angles 2θ from 5° to 40° with increments of $1^\circ/\text{min}$. The X-ray images were analysed using the Shimadzu PC XRD software (version 7.04) and the PDF2 database (version 2.2201). Crystallinity was calculated using the Shimadzu Crystallinity software (version 7.04), taking into account the halo in the range of 15° - 30° , which is characteristic of the amorphous phase.

The morphology and crystal size of the samples were analysed using scanning electron microscopy (SEM) using a Hitachi Regulus SU8220 microscope. Images were taken in the secondary electron mode with an acceleration voltage of 5 kV. Prior to imaging, the samples were positioned on a 25 mm diameter aluminium stage and secured with conductive carbon tape.

Characteristics of the porous structure, including BET specific surface area, the volume of micro-, meso-, and macropores, were measured using low-temperature N_2 adsorption-desorption on a Quantachrome Nova 1200e sorption meter and mercury porosimetry using a Carlo Erba Porosimeter-2000.

The volume of micropores in the presence of mesopores was calculated using the t-plot method. The pore size distribution was determined using the BJH model (Halenda). Mercury penetration into pores with radii ranging from 30 to 10000 Å was carried out under pressures ranging from 0.1 to 200 MPa. During data processing, differential curves for the distribution of pores over radii were obtained, from which the contributions of pores of different sizes to the total volume of the porous space of the catalyst were determined.

The acid site types and concentrations were determined by IR spectroscopy after pyridine adsorption (IR-Py). IR spectra of the adsorbed pyridine were recorded using a Bruker Vertex-70V IR spectrometer (Bruker Optic GmbH, Ettlingen, Germany) with a resolution of 4 cm^{-1} . The samples were precalcined at 450°C for 2 h in a 10^{-2} Pa vacuum. Pyridine was adsorbed onto the molecular sieve samples at 150°C for 30 min. Pyridine was desorbed at 150°C , 250°C , and 350°C . The concentrations of Brønsted acid sites (BAS) and Lewis acid sites (LAS) were calculated by integrating the absorbance bands at 1545 cm^{-1} and 1454 cm^{-1} , respectively, using a previously described method [21].

The mechanical strength of the granular samples was tested on the Lintel PC-21 machine under static conditions using the compression method. Cylindrical granules with a length of 5-6 mm and a diameter of 1.4-1.6 mm were tested according to the ASTM D6175 standard.

2.9. Methods for Testing Catalysts

The catalytic transformations of n-hexadecane ($\text{H-C}_{16}\text{H}_{34}$, 99%, Acros Organics) were studied in a flow reactor at temperatures between 220 and 260°C and a pressure of 3 MPa. A molar ratio of $\text{H}_2/\text{H-C}_{16}\text{H}_{34}=10$ was used, and the mass feed rate was 2 h^{-1} . The reaction products were analyzed by gas-liquid chromatography on a Chromatek-Crystal 5000 chromatograph with a flame ionization detector and a glass capillary column (50 m, HP-1). Chromato-mass spectrometry was also used, with a Shimadzu instrument whose chromatograph was equipped with a DB-5 column (50 m).

3. Results and Discussion

The catalytic properties of ZSM-5 zeolite depended on the degree of crystallinity and the presence of impurity phases. Figure 1 shows X-ray images of powdered ZSM-5 zeolite, amorphous aluminosilicates, granules containing amorphous aluminosilicates and boehmite, and granules of ZSM-5 zeolite without binder.

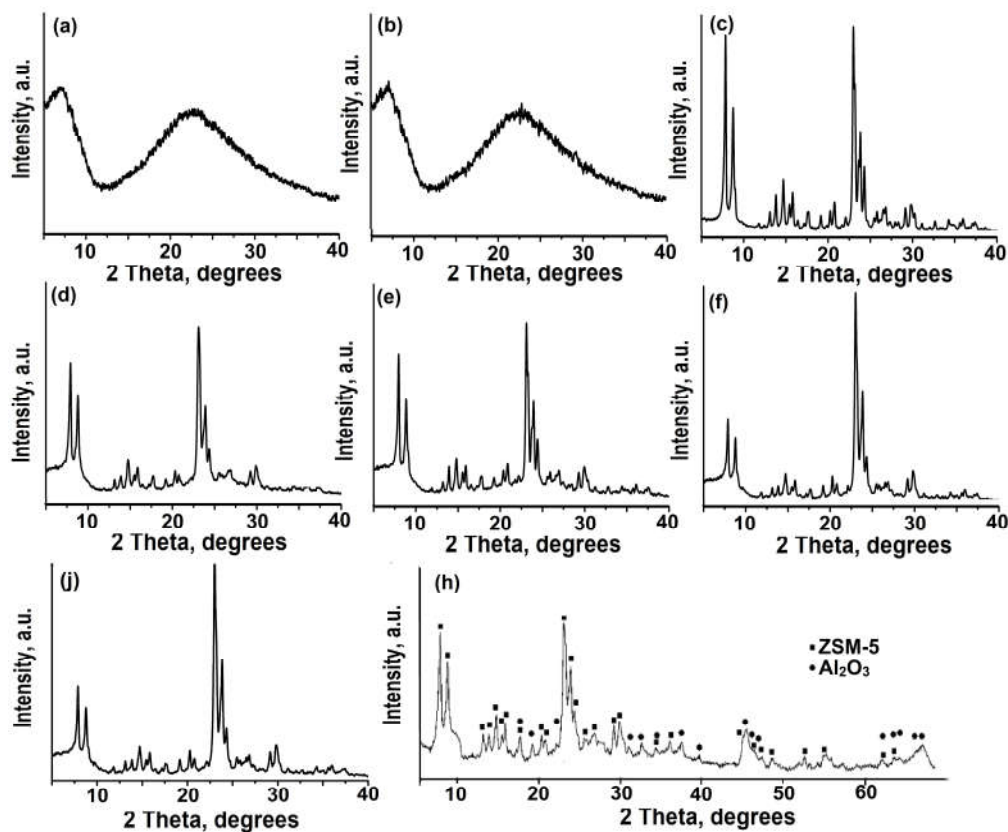


Figure 1. X-ray diffraction of powdered and granular samples: (a) – ASM-1; (b) – ASM-2; (c) – NaZSM-5; (d) – NaZSM-5-ASM-1; (e) – NaZSM-5-ASM-2; (f) – NaZSM-5-WB-1; (g) – NaZSM-5-WB-2; (h) – NaZSM-5-BD.

It can be seen from the X-ray diffraction pattern of the NaZSM-5 zeolite powder sample that there are several intense signals at specific angles: 7.92°, 8.94°, 23.04°, 23.38° and 23.94° degrees 2θ. These specific angles are characteristic of the MFI crystal structure with high phase purity (PDF №00-037-0390).

Amorphous aluminosilicates show a strong diffraction peak in the 2θ angle range of 15-30°, regardless of the silicon source used. Granular samples containing ZSM-5 zeolite and amorphous aluminosilicates show a well-defined diffraction peak in the 20-30° angle range, with a degree of crystallinity that does not exceed 70% for these granules.

After crystallization, the amorphous phase in the granules transforms into ZSM-5 zeolite with a high degree of purity and a crystallinity of at least 95%. The results indicate that the granular sample has a similar level of crystallinity to that of powdered ZSM-5 zeolite.

Table 1 shows the results of a study of the chemical composition of amorphous aluminosilicates and powdered and granular ZSM-5 zeolites. The SiO₂/Al₂O₃ ratio in powdered NaZSM-5 zeolite was found to be slightly lower than in the reaction mixture, due to incomplete aluminium incorporation during crystallization. This is in contrast to amorphous aluminosilicates, where the SiO₂/Al₂O₃ ratio was closer to the calculated value.

In granular samples, the SiO₂/Al₂O₃ ratios are also similar before and after crystallization, indicating that the SiO₂/Al₂O₃ ratio of amorphous aluminosilicates and zeolite ZSM-5 crystals remains constant during synthesis. However, in the granular sample of NaZSM-5-BD zeolite, there is a decrease in the SiO₂/Al₂O₃ ratio due to the addition of boehmite to the granules.

Table 1. Chemical composition of amorphous aluminosilicates, powdered and granular ZSM-5 zeolites.

Sample	Chemical composition, wt. %			SiO ₂ /Al ₂ O ₃ molar ratio
	Na ₂ O	Al ₂ O ₃	SiO ₂	
ASM-1	0	5.6	94.4	29
ASM-2	3.2	5.3	91.5	29

NaZSM-5	2.0	3.3	94.7	49
NaZSM-5-ASM-1	1.2	4.2	94.6	38
NaZSM-5-ASM-2	2.5	4.0	93.5	39
NaZSM-5-WB-1	2.0	3.4	94.6	47
NaZSM-5-WB-2	2.0	3.4	94.6	47
Na-ZSM-5-BD	1.5	22.7	75.8	6

The morphology and size of zeolite crystals is also one of the key factors affecting their catalytic properties [22]. Figure 2 shows scanning electron microscope (SEM) images of amorphous aluminum silicates obtained using different silicon sources. These images show that amorphous aluminosilicates are xerogels composed of spherical particles. ASM-1 aluminosilicate, obtained using TEOS, has particles with a size between 5 and 10 nm, whereas ASM-2, obtained using an inorganic silicon source, is characterized by larger particles with a size between 10 and 20 nm.

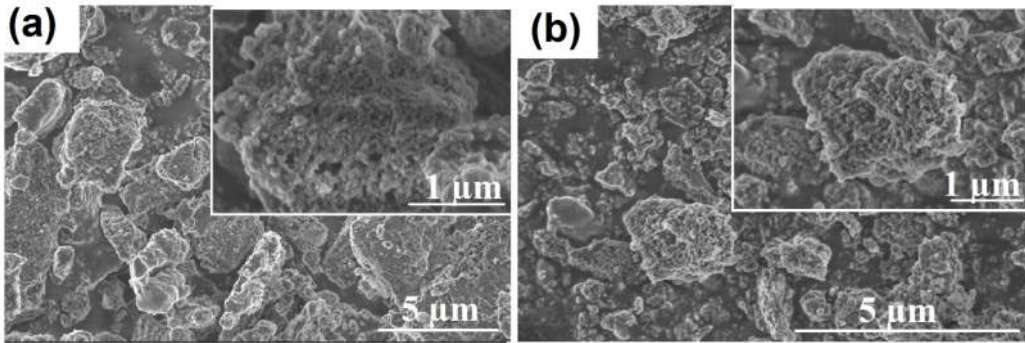


Figure 2. SEM images of samples of amorphous aluminosilicates: (a) – ASM-1; (b) –ASM-2.

According to the SEM data (Figure 3), the powdered NaZSM-5 sample consists of crystals in the form of fused prisms with sizes ranging from 300 to 500 nm. The NaZSM-5-ASM-1 and NaZSM-5-ASM-2 granules produced from the Na-ZSM-5 sample, are composite materials composed of Na-ZSM-5 molecular sieve crystals with sizes ranging from 300 to 500 nm and highly dispersed particles of amorphous aluminosilicate filling the spaces between the crystals. The granules of the NaZSM-5-WB-1 and NaZSM-5-WB-2 zeolite samples are composed of clusters of crystals with different morphologies. These crystals can be cubic in shape with a size between 50 and 200 nm or elongated prismatic in shape with a size between 300 and 500 nm. It is worth noting that the NaZSM-5-WB-1 zeolite sample contains crystals that are smaller in size compared to those in the NaZSM-5-WB-2 zeolite sample. The results obtained can be explained by the fact that during the crystallization of granules containing ASM-1 aluminosilicate, a higher degree of supersaturation of crystal nuclei is created compared to the crystallization of granules containing ASM-2 aluminosilicate. This results in the formation of more finely dispersed crystals.

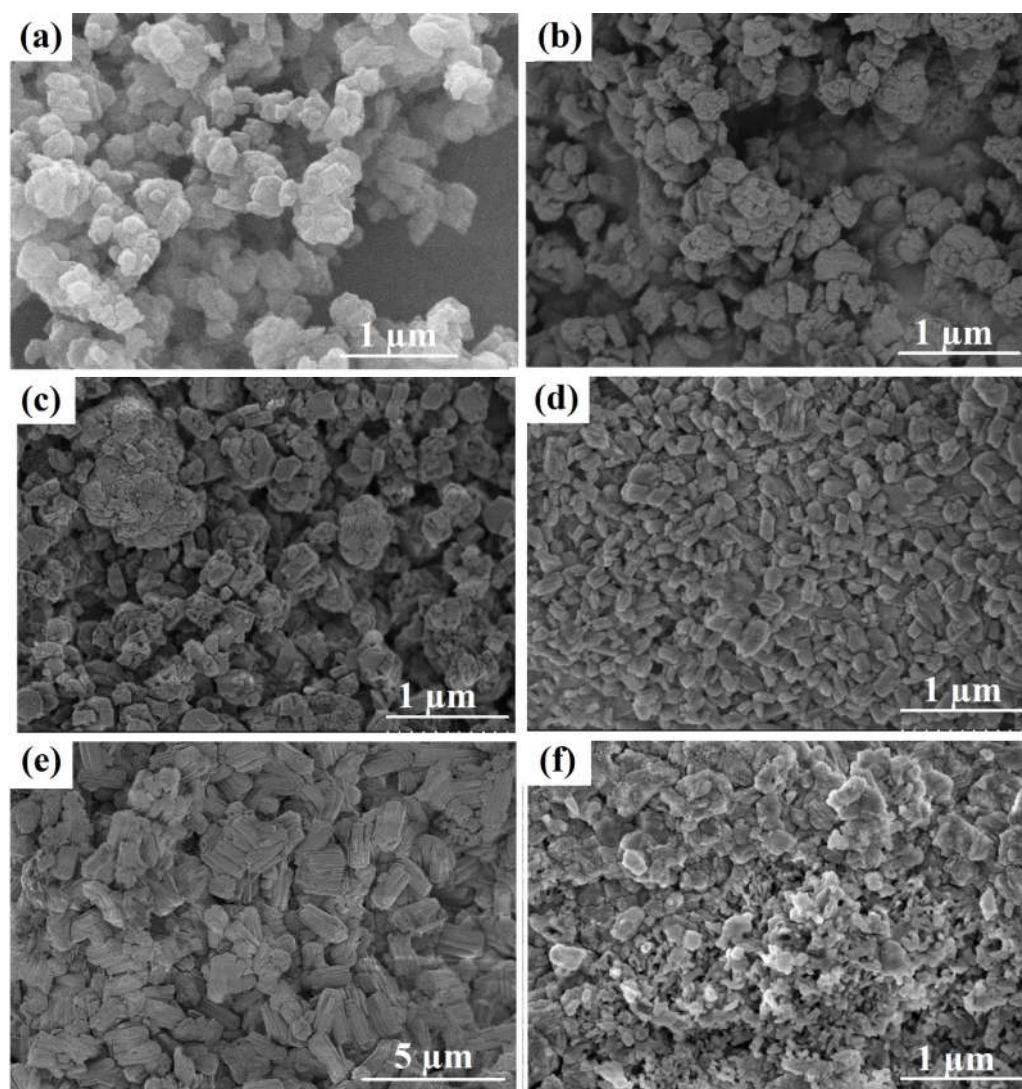


Figure 3. SEM images of samples of powdered and granular ZSM-5 zeolites: (a) – Na-ZSM-5; (b) – NaZSM-5-ASM-1; (c) –NaZSM-5-ASM-2; (d) –NaZSM-5-WB-1; (e) –NaZSM-5-WB-2; (f) – Na-ZSM-5-BD.

The NaZSM-5-BD zeolite sample consists of ZSM-5 molecular sieve crystals, with crystal sizes ranging from 300 to 500 nm, and highly dispersed aluminium oxide particles filling the spaces between the crystals.

Figure 4 shows photographs of granules both before and after the crystallization process. It is clear that the crystallization had little or no effect on the appearance or size of the granules.

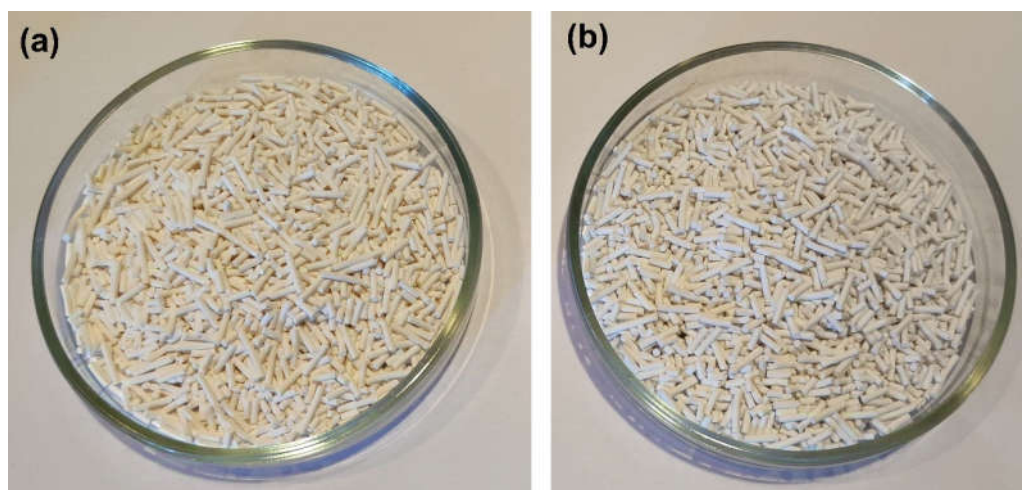


Figure 4. Photo of granules before and after crystallization:(a) –NaZSM-5-ASM-1; (b) - NaZSM-5-WB-1.

Granular industrial catalysts based on ZSM-5 zeolite require high mechanical strength, as large amounts of catalyst in the reactor can cause the lower layers to collapse under the pressure of their own weight.

Table 2 presents data on the mechanical strength results of ZSM-5 zeolite granules after the crystallization process. The strength of the granules increased by 2-3 times after crystallization compared to granules with amorphous aluminosilicates. This is due to the fusion of zeolite crystals from the initial granules with crystals formed during the crystallization of the amorphous component in the granules. As we mentioned previously, these granular materials form a single structure of fused crystals [19]. The NaZSM-5-WB-1 sample has a higher mechanical strength than the NaZSM-5-WB-2 sample, due to the fact that its initial granules contain aluminosilicates with a more uniform particle distribution. This leads to an increase in the contact surface area and a denser crystal fusion, resulting in an increase in strength.

Table 2. Mechanical strength of granular ZSM-5 zeolite samples.

Sample	Mechanical Crushing Strength (Radial)		Mechanical Crushing Strength (Uniaxial), N/mm ²
	N/pellet	N/mm ²	
NaZSM-5-ASM-1	19±4	4±1	5±1
NaZSM-5-ASM-2	17±3	3±1	4±1
NaZSM-5-WB-1	60±14	11±3	12±3
NaZSM-5-WB-2	58±13	9±2	10±2
Na-ZSM-5-BD	43±9	7±1	8±2

Results are shown as the mean ± standard deviation, SD (n = 24).

Comparing the mechanical strength of the NaZSM-5-WB and NaZSM-5-BD granules, it can be observed that the strength of the samples with a hierarchical porous structure is approximately 20% higher, due to the unique formation process.

Figure 5 shows the nitrogen adsorption-desorption isotherms and the pore size distribution for all samples. It can be seen that all isotherms are close to type IV, with a sharp increase in the low pressure region and a hysteresis loop of type H3 between 0.8 and 1.0 pressure. This type of isotherm is typical of micro-mesoporous materials. The formation of mesopores in NaZSM-5 is due to the partial melting of nanoscale crystals into prism-like structures, as can be clearly seen from the SEM images (Figure 3).

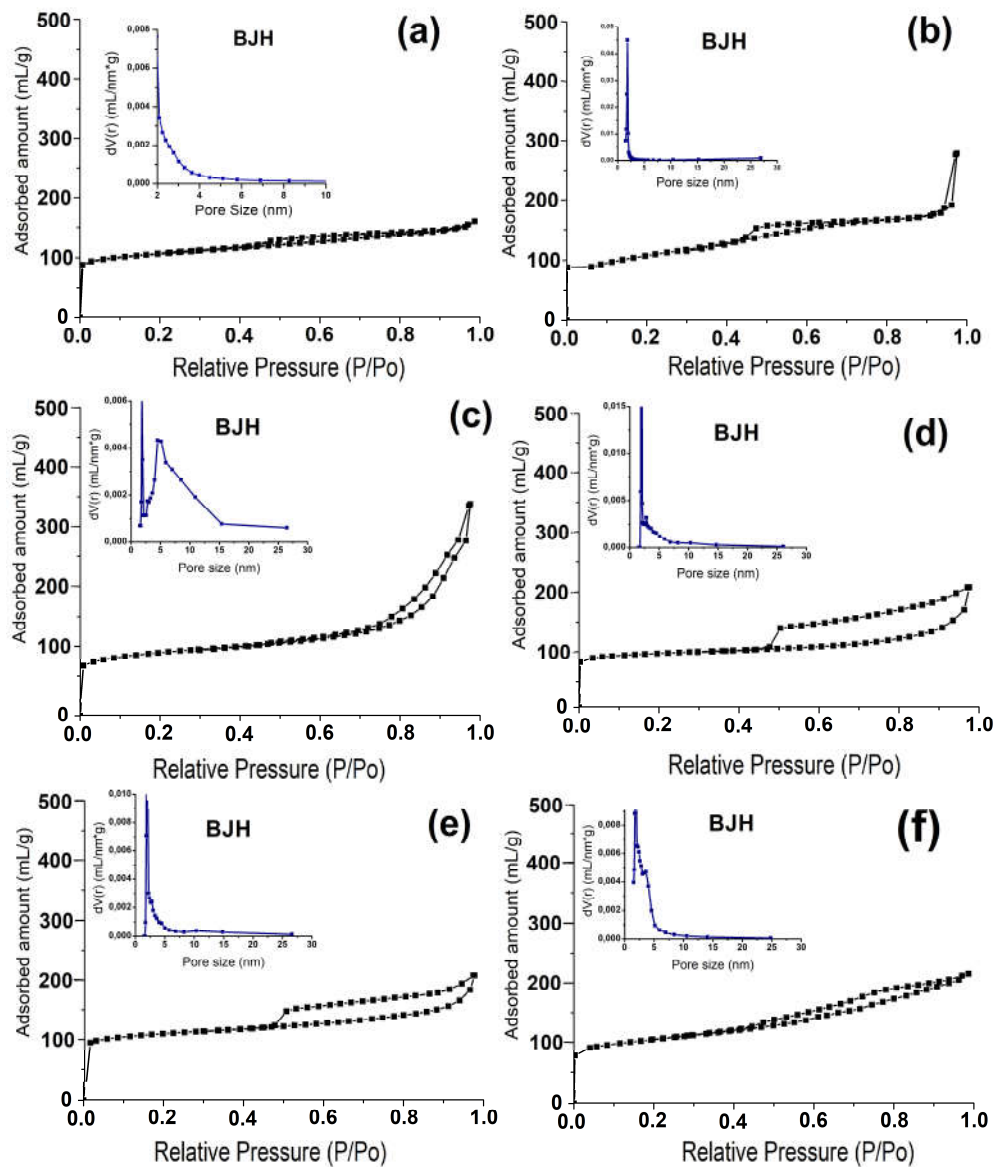


Figure 5. Nitrogen adsorption–desorption isotherms and pore size distribution of (BJH) for granular and powdered zeolite samples of ZSM-5: (a) –Na-ZSM-5; (b) –NaZSM-5-ASM-1; (c) –NaZSM-5-ASM-2; (d) –NaZSM-5-WB-1; (e) –NaZSM-5-WB-2; (f) –Na-ZSM-5-BD.

Table 3 shows the characteristics of the porous structure of powdered zeolite and granules made from it. It can be seen that the introducing of ~40% by weight of amorphous aluminosilicate into the granules (NaZSM-5-ASM-1 zeolite sample) results in a decrease of about 30% in the volume of micropores and an increase in the volume of mesopores. This decrease in micropore volume and increase in mesopore volume is due to the addition of mesoporous amorphous aluminosilicate to the composition. The NaZSM-5-ASM-1 sample has a higher specific surface area and mesopore volume than the NaZSM-5-ASM-2 sample. This is because the former contains an aluminosilicate with a smaller particle size. After crystallization, granular samples experience an increase in micropore volume due to the formation of ZSM-5 zeolite crystals.

Table 3. Characteristics of the porous structure of granular and powdered ZSM-5 zeolite samples.

Sample	$S_{BET}, m^2/g$	$V_{micro}, cm^3/g$	$V_{meso}, cm^3/g$	$HgV_{macro}, cm^3/g$
Na-ZSM-5	285	0.12	0.01	-
NaZSM-5-ASM-1	363	0.06	0.37	0.35
NaZSM-5-ASM-2	353	0.06	0.30	0.30

NaZSM-5-WB-1	347	0.11	0.28	0.27
NaZSM-5-WB-2	329	0.11	0.20	0.21
Na-ZSM-5-BD	276	0.07	0.09	0.28

S_{BET} - specific surface according to BET. V_{micro} - specific volume of micropores. V_{meso} - specific volume of mesopores. HgV_{macro} - specific volume of macropores.

The specific surface area and volume of mesopores in the NaZSM-5-WB-1 sample are higher than those in the NaZSM-5-WB-2 sample, due to the smaller crystals formed in its granules. In a granular sample containing a boehmite-based binder, there is a decrease in the specific surface area and volume of micropores due to the presence of the binder in the granules.

A higher volume of macropores was observed for the NaZSM-5-WB-2 zeolite sample compared to the NaZSM-5-WB-1 sample. This is due to the presence of larger crystals in the granules of the NaZSM-5-5-WB2 sample. Among the granular samples, the ZSM-5 samples without binders were characterized by the highest volume of macropores. Therefore, granular samples without binders can be considered as hierarchical materials in which a well-developed secondary porous structure consisting of meso- and macropores has formed.

The acidic properties of H-ZSM-5 zeolite samples were investigated by IR spectroscopy of pyridine adsorption (Figure 6). The bands at 1636 and 1546 cm^{-1} correspond to pyridine adsorbed on Brønsted acid sites (BAS). The bands at 1623, 1454 and 1384 cm^{-1} in HZSM-5-WB-1 (Figure 6b), HZSM-5-WB-2 (Figure 6c) and HZSM-5-BD-1 (Figure 6d) zeolite samples correspond to pyridine adsorbed on Lewis acid sites in zeolite (LAS). Samples HZSM-5-WB-1, HZSM-5-WB-2, and HZSM-5-BD show bands at 1614, 1601, and 1447 cm^{-1} , respectively, which are associated with adsorption on weak Lewis acid sites on frameless aluminium. The band at 1490 cm^{-1} is attributed to both BAS and LAS.

The sample based on the original powdered ZSM-5 in H-form is mainly characterised by the presence of Brønsted acidity. Table 4 shows that the BAS content is 295 $\mu mol/g$, and the LAS content is 39 $\mu mol/g$. The total BAS concentration of the H-ZSM-5-WB-1 zeolite is higher than that of the original H-ZSM-5 powder at 318 $\mu mol/g$. However, the amount of strong basic sites (desorption at 350°C) is the same. This can be explained by the fact that the H-ZSM-5-WB-1 granular sample has a higher crystal dispersion and specific surface area and a higher concentration of acid sites.

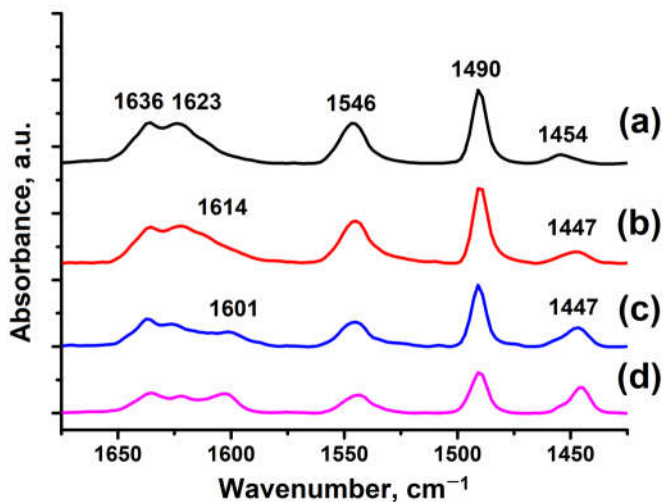


Figure 6. IR spectra of adsorbed pyridine for granular and powdered ZSM-5 zeolite samples: (a) HZSM-5, (b) HZSM-5-WB-1, (c) HZSM-5-WB-2, and (d) HZSM-5-BD.

Table 4. Concentrations of acid sites in granular and powdered ZSM-5 zeolite samples according to IR spectroscopy data with pyridine adsorption.

Sample	Acidity (μmol/g)					
	BAS			LAS		
	150 °C	250 °C	350 °C	150 °C	250 °C	350 °C
H-ZSM-5	295	256	223	39	25	24
H-ZSM-5-WB-1	318	278	224	59	27	16
H-ZSM-5-WB-2	206	173	132	90	34	15
H-ZSM-5-BD	148	124	99	106	39	17

The H-ZSM-5-WB-2 zeolite sample shows a decrease in the number of BAS to 206 μmol/g and an increase in the number of LAS to 90 μmol/g. The majority of these are weak Lewis acid sites (desorbing up to 250°C). It is likely that there is more amorphous aluminosilicate present in the composition of H-ZSM-5-WB-2 than in H-ZSM-5-WB-1, as almost all of the amorphous component has crystallized in the latter.

Similarly, an even greater decrease in BAS concentration to 148 μmol/g in the H-ZSM-5-BD granular sample is associated with the dilution of the ZSM-5 γ-Al₂O₃ zeolite. Apparently, γ- Al₂O₃ simultaneously acts as a source of weak LAS, and therefore an increase in the LAS concentration to 106 μmol/g is observed.

As a result of testing the catalytic properties of Pt/ZSM-5 zeolite samples in the hydroconversion of n-hexadecane, we found that the highest activity was exhibited by a sample of Pt/ZSM-5-WB-1 with the highest concentration of BAS. The Pt/ZSM-5-BD zeolite sample with the lowest BAS concentration was the least active in the hexadecane hydroconversion process. At 220 °C, the hexadecane conversion was 59.1%, 50.2% and 31.5% for the Pt/ZSM-5-WB-1, Pt/ZSM-5-WB-2, and Pt/ZSM-5-BD zeolite samples, respectively.

It has been found that the main reaction pathway for the conversion of hexadecane over Pt/ZSM-5 catalysts is hydrocracking (Figure 7), which produces hydrocarbons with carbon numbers ranging from 5 to 10 as the main products (Table 5). As the reaction temperature is increased from 220 to 260 °C, the yield of gaseous C₂-C₄ hydrocarbons increases, while the content of C₁₁-C₁₃ hydrocarbons decreases. At the same time, there is a decrease in the concentration of normal-structure hydrocarbons relative to iso-structure hydrocarbons (i/n ratio).

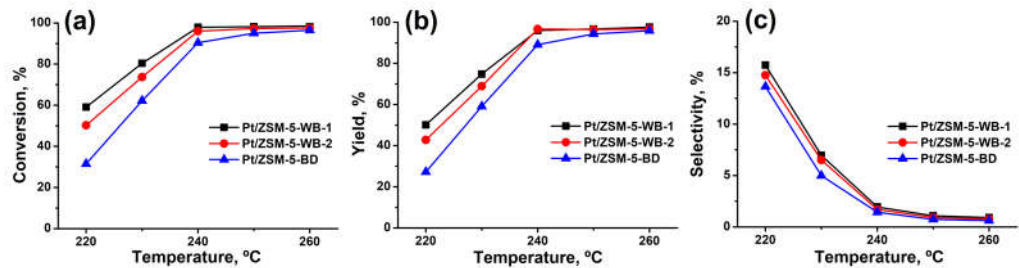


Figure 7. Catalytic transformations of n-hexadecane on Pt/ZSM-5 zeolite samples: (a) - Dependence of the conversion of n-hexadecane on the reaction temperature; (b) - Dependence of the yield of cracking products on the reaction temperature; (c) - Dependence of the selectivity for formation of hexadecane isomers on the reaction temperature.

Another direction of hexadecane conversion using Pt/ZSM-5 catalyst samples is hydroisomerization (Figure 7). The Pt/ZSM-5-WB-1 sample, which has a higher crystal dispersion, shows the highest selectivity for hexadecane isomers. At 220 °C, the selectivity for hexadecane isomer formation on the Pt/ZSM-5-WB-1, Pt/ZSM-5-WB-2, and Pt/ZSM-5-BD samples was 13.6%, 14.8% and 15.7%, respectively.

Table 5. Yield of n-hexadecane hydrocracking products on Pt/ZSM-5 samples and the ratio of normal and isoparaffins with a carbon chain length between 5 and 13 carbon atoms (i/n).

Sample	Temperature, °C	Yield, wt. %			i/n
		C ₂ -C ₄	C ₅ -C ₁₀	C ₁₁ -C ₁₃	
Pt/ZSM-5-WB-1	220	13.8	32.7	3.6	0.9
	240	29.7	64.1	2.2	1.2
	260	34.1	62.2	1.2	1.8
Pt/ZSM-5-WB-2	220	11.5	28.1	3.2	0.7
	240	31.6	60.5	1.9	1.0
	260	35.5	59.9	1.0	1.5
Pt/ZSM-5-BD	220	8.4	11.9	2.6	0.4
	240	32.3	54.0	1.5	0.8
	260	37.9	56.6	0.8	1.3

4. Conclusions

The physicochemical properties of the products of crystallization of granules (containing 60% by weight of powdered ZSM-5, and 40% by weight of a temporary binder) into granular zeolite using the "less-bind" technology were studied by XRD, XRF, SEM, N₂ adsorption-desorption, mercury porometry, and IR spectroscopy with pyridine adsorption.

Two amorphous aluminosilicates with a SiO₂/Al₂O₃ molar ratio of 50 were used as a temporary binders. One was prepared from tetraethyl orthosilicate and aluminium nitrate by a two-step sol-gel process, while the other was prepared from aqueous solutions of sodium silicate and aluminium sulphate.

It was found that during the crystallization process, granules prepared using amorphous aluminosilicates as a temporary binder yielded granular ZSM-5 zeolites (d=1.5 mm, l= 5 mm) with high phase purity and a hierarchical porous structure. The specific surface area of these granules was found to be between 330 and 350 m²/g, with mesopore volumes between 0.20 and 0.28 cm³/g and macropore volumes between 0.20 and 0.30 cm³/g.

It has been found that during the crystallization of granules containing amorphous aluminosilicate, with a larger specific surface area and smaller particle size, nanoscale crystals of ZSM-5 zeolite are formed, which are smaller in size.

It has been shown that granular ZSM-5 zeolites with high phase purity and a hierarchical porous structure outperform granular ZSM-5 zeolites with an aluminum oxide binder in terms of mechanical strength.

It was found that a bifunctional catalyst is formed on the H-form of granular ZSM-5 zeolite with a high degree of crystallinity and a hierarchical porous structure when 0.5 wt% Pt is added. This catalyst exhibits higher activity and selectivity in the hydroisomerization of n-hexadecane compared to a catalyst prepared using granular ZSM-5 zeolite with a binder.

Author Contributions: Author Contributions: Conceptualization, M.R.A.; Methodology, M.R.A., O.S.T., B.I.K.; Validation, M.R.A., O.S.T.; Investigation, M.R.A.; O.S.T.; N.A.F.; A.I.M. and D.V.S., A.K.I.; R.A.Z.; Writing—Original Draft Preparation, M.R.A., N.A.F.; Writing—Review & Editing, M.R.A., N.A.F., O.S.T. and D.V.S.; Resources, A.K.I.; R.A.Z.; N.A.F., D.V.S.; Visualization, N.A.F.; Supervision, M.R.A., B.I.K. Funding Acquisition, B.I.K.; M.R.A. All authors have read and agreed to the published version of the manuscript.

Funding: This study was performed under a state task to Institute of Petrochemistry and Catalysis UFRS RAS (subject no. FMRS-2024-0012 «Bifunctional Molecular-Sieve Catalytic Systems for the Production of Low-Pour-Point Diesel Fuels»).

Institutional Review Board Statement: Not applicable.

Informed Consent Statement: Not applicable.

Data Availability Statement: The original contributions presented in the study are included in the article, further inquiries can be directed to the corresponding authors.

Conflicts of Interest: The authors declare no conflict of interest.

References

1. Primo, A.; Garcia, H. Zeolites as catalysts in oil refining. *Chem. Soc. Rev.* **2014**, *43*, p. 7548–7561. [https://doi.org/10.1039/C3CS60394F]
2. Vermeiren, W.; Gilson, J.P. Impact of zeolites on the petroleum and petrochemical industry. *Top. Catal.* **2009**, *52*, pp. 1131–1161. [DOI: 10.1007/s11244-009-9271-8]
3. Database of Zeolite Structure. Available online: <http://www.iza-structure.org/databases> (accessed on 20 January 2024).
4. Konnov, S. V.; Dubray, F.; Clatworthy, E.B.; Kouvatas, C.; Gilson, J.-P.; Dath, J.-P.; Minoux, D.; Aquino, C.; Valtchev, V.; Moldovan, S.; Koneti, S.; Nesterenko, N.; Mintova, S. Novel Strategy for the Synthesis of Ultra-Stable Single-Site Mo-ZSM-5 Zeolite Nanocrystals *Angewandte Chemie*. **2020**, *132*, *44*, pp. 19721–19728. [https://doi.org/10.1002/ange.202006524]
5. Meng, L.; Zhu, X.; Hensen, J. M. Stable Fe/ZSM-5 Nanosheet Zeolite Catalysts for the Oxidation of Benzene to Phenol. *ACS Catalysis*. **2017**, *7*, *4*, pp. 2709–2719. [doi.org/10.1021/acscatal.6b03512]
6. Jia, C.; Zong, L.; Wen, Y.; Xu, H.; Wei, H. & Wang, X. Synthesis and scale-up of ZSM-5 aggregates with hierarchical structure. *Res Chem Intermed*, **2019**, *45*, pp. 3913–3927. [https://doi.org/10.1007/s11164-019-03828-x]
7. Jia, Y.; Shi, Q.; Wang, J.; Ding, C. & Zhang, K. Synthesis, characterization, and catalytic application of hierarchical nano-ZSM-5 zeolite. *RSC advances*, **2020**, *10*, *50*, pp. 29618–29626. [DOI: 10.1039/D0RA06040B]
8. Zhang, C.; Fan, K.; Ma, G.; Lei, C.; Xu, W.; Jiang, J.; Sun, B.; Zhang, H.; Zhu, Y.; Wen, S. Efficient Synthesis of Mesoporous Nano ZSM-5 Zeolite Crystals without a Mesoscale Template. *Crystals* **2021**, *11*, p. 1247. [https://doi.org/10.3390/cryst11101247]
9. Zheng, Y.; Ning, W.; Wang, Q.; Wei, X.; Li, X.; Pan, M. Hierarchical ZSM-5 zeolite using amino acid as template: Avoiding phase separation and fabricating an ultra-small mesoporous structure. *Microporous and Mesoporous Materials*, **2023**, *355*, p. 112578. [https://doi.org/10.1016/j.micromeso.2023.112578]
10. Shen, Y.; Li, H.; Zhang, X.; Wang, X.; Lv, G. The diquaternary ammonium surfactant-directed synthesis of single-unit-cell nanowires of ZSM-5 zeolite. *Nanoscale*, **2020**, *12*, *10*, pp. 5824–5828. [https://doi.org/10.1039/D0NR00424C]
11. Wang, P.; Xiao, X.; Pan, Y.; Zhao, Z.; Jiang, G.; Zhang, Z.; Meng, F.; Li, Y.; Fan, X.; Kong, L. Facile Synthesis of Nanosheet-Stacked Hierarchical ZSM-5 Zeolite for Efficient Catalytic Cracking of n-Octane to Produce Light Olefins. *Catalysts*, **2022**, *12*, p. 351. [https://doi.org/10.3390/catal12030351]
12. Tajuddin, N. A.; Kamal, N. A.; Rhymme, N. A. Q.; Sani, S. F. Hierarchical Zeolite Zsm-5 Framework On The Synthesis And Characterization For Catalytic Cracking Of Fluid: A Mini Review. *Malaysian Journal Of Analytical Sciences*, **2023**, *27*, *3*, pp. 499–509.
13. Hao, J.; Zhou, J.; Wang, Y.; Li, L.; Sheng, Z.; Teng, J.; Xie, Z. Pore mouth catalysis promoting n-hexane hydroisomerization over a Pt/ZSM-5 bifunctional catalyst. *Chem Catalysis*, **2024**, *4*, *8*, p. 101041. [DOI: 10.1016/j.checat.2024.101041]
14. Yang, N.; Fu, T.; Cao, C.; Wu, X.; Zheng, H.; Li, Z. Constructing hierarchical ZSM-5 coated with small ZSM-5 crystals via oriented-attachment and in situ assembly for methanol-to-aromatics reaction. *Front. Chem. Sci. Eng.* **2024**, *18*, p. 76. [https://doi.org/10.1007/s11705-024-2432-2]
15. He, X.; Tian, Y.; Qiao, C.; Liu, G. Acid-driven architecture of hierarchical porous ZSM-5 with high acidic quantity and its catalytic cracking performance. *Chemical Engineering Journal*, **2023**, *473*, p. 145334. [https://doi.org/10.1016/j.cej.2023.145334]
16. Asgar Pour, Z.; Abduljawad, M.M.; Alassmy, Y.A.; Cardon, L.; Van Steenberge, P.H.M.; Sebakhy, K.O. A Comparative Review of Binder-Containing Extrusion and Alternative Shaping Techniques for Structuring of Zeolites into Different Geometrical Bodies. *Catalysts* **2023**, *13*, p. 656. [https://doi.org/10.3390/catal13040656]

17. Bingre, R.; Louis, B.; Nguyen, P. An Overview on Zeolite Shaping Technology and Solutions to Overcome Diffusion Limitations. *Catalysts* **2018**, *8*, p. 163. [<https://doi.org/10.3390/catal8040163>]
18. Fakin, T.; Ristić, A.; Mavrodinova, V.; Logar, N.Z. Highly crystalline binder-free ZSM-5 granules preparation. *Microporous Mesoporous Mater.* **2015**, *213*, pp. 108–117. [[10.1016/j.micromeso.2015.04.010](https://doi.org/10.1016/j.micromeso.2015.04.010)]
19. Travkina, O.S.; Agliullin, M.R.; Filippova, N.A.; Khazipova, A.N.; Danilova, I.G.; Grigor'eva, N.G.; Narenderd, N.; Pavlov M.L.; Kutepov B.I. Template-free synthesis of high degree crystallinity zeolite Y with micro-meso-macroporous structure. *RSC Adv.*, **2017**, *7*, pp. 32581-32590. [<https://doi.org/10.1039/C7RA04742H>]
20. Agliullin, M.R.; Danilova, I.G.; Faizullin, A.V.; Amarantov, S.V.; Bubenov, S.V.; Prosochkina, T.R.; Grigor'eva, N.G.; Paukshtis, E.A.; Kutepov B.I. Sol-gel synthesis of mesoporous aluminosilicates with a narrow pore size distribution and catalytic activity thereof in the oligomerization of dec-1-ene. *Microporous and Mesoporous Materials* **2016**, *230*, pp. 118-127. [<https://doi.org/10.1016/j.micromeso.2016.05.007>]
21. Tamura M.; Shimizu K.-I.; Satsuma A. Comprehensive IR study on acid/base properties of metal oxides. *Appl. Catalysis A: General.* **2012**, *433*, pp. 135-145. <https://doi.org/10.1016/j.apcata.2012.05.008>.
22. Li, S.; Li, J.; Dong, M.; Fan, S.; Zhao, T.; Wang J.; Fan, W. Strategies to control zeolite particle morphology. *Chem Soc Rev.* **2019**, *48*, pp. 885-907. [DOI: 10.1039/c8cs00774h]

Disclaimer/Publisher's Note: The statements, opinions and data contained in all publications are solely those of the individual author(s) and contributor(s) and not of MDPI and/or the editor(s). MDPI and/or the editor(s) disclaim responsibility for any injury to people or property resulting from any ideas, methods, instructions or products referred to in the content.